AIAA-2000-1696

THE PRACTICAL IMPLEMENTATION OF NON-CONTACTING LASER STRAIN MEASUREMENT SYSTEMS

Isam Yunis*
Mission Analysis Branch/VB-A3
Expendable Launch Vehicles
Kennedy Space Center, FL 32899

Roger D. Quinn† and Jaikrishnan R. Kadambi‡
Department of Mechanical and Aerospace Engineering
Case Western Reserve University
Cleveland, OH 44106

ABSTRACT

Measurement of stress and strain in rotating turbomachinery is critical to many industries. The search for a non-contacting, non-interfering, non-degrading measurement system is on going and extensive. While several methods seem promising in theory, implementation has proven troublesome. This work uncovers and quantifies these implementation issues in the context of a laser measurement system. Both a Laser Doppler Velocimeter system and a displacement laser system are utilized. It is found that the key issues are signal to noise ratio, rigid body compensation, measurement location, and conversion of intermittent measurements to a continuous signal. Accounting for these factors leads to successful measurements. These results should lead to better ideas and more practical solutions to the non-contacting, non-degrading, non-interfering strain measurement system problem.

INTRODUCTION

The dynamics of rotating blades has been an important research topic for decades.[1] Many industries use rotating blades. The aircraft industry is the most prevalent with its use of ducted fans, multi-stage turbines and compressors, propellers, and helicopter rotors. However, other industries such as the power industry, the boat engine manufacturers, and the windmill industry have a vested interest in the advancements in blade dynamics. It is not surprising then that blade analysis and testing have been the subjects of voluminous research, especially in the last two decades. While blade theory and finite element analysis of blades is important and often very accurate, it is testing that ultimately garners trust in the complicated problem of rotating blades.

Much of the work in improving the testing of rotating blades has been in order to develop a non-contacting, non-degrading, and non-interfering methodology and tool to sense frequency variations, to sense mode shape variations, to measure vibrations, and to measure the stress history of the blade[2,3,4,5,6,7,8,9]. In essence, the search is for a means to record the vibration history of the blade. Some of these theories and systems have been implemented and demonstrated, but all have failed in all but the most basic demonstrations. Overcoming the implementation issues remains paramount.

Recently the Laser Doppler Velocimeter (LDV) surfaced as a candidate for the dynamic measurement of rotating blades.[10,11] Reinhardt et al. showed that the method is viable for the accurate measurement of the vibrations of rotating flat plates. However, the authors only demonstrated the technique for the insignificant case of a blade with a much higher vibration frequency than rotation frequency. It remains to show that this system works for more realistic rotation speeds, for non-resonant excitation, and that strain can be resolved from an intermittent velocity signal.

Using Reinhardt as a springboard, this work

* Aerospace Engineer, Senior Member AIAA
† Professor, Senior Member AIAA, ASME
‡ Professor, Fellow ASME

presents a non-contacting, non-degrading strain measurement method using laser systems. The method is a multi-mode measurement approach for use during fan operation. Displacement lasers and laser vibrometers are used in the development, although displacement lasers prove more viable. Most importantly, several key practical implementation issues identified and resolved. These issues are signal to noise ratio, rigid body compensation, measurement location, and conversion of intermittent measurements to a continuous signal. These issues are of universal importance to and key in the demonstration of any similar system.

LASER MEASUREMENT HARDWARE

Displacement Lasers

Since, hardware limitations govern most practical issues, a discussion of the laser hardware is a logical starting point. In recent years, the development of displacement lasers has progressed at a significant rate. The resolution of such instruments can be very high, on the order of 10^{-6} inches. This accuracy is ideally suited for measuring small blade vibrations with high accuracy. Also, the quality of the signal is exceedingly clear.

The drawback of displacement lasers today is that these high accuracies are achieved by very short offset distances. Typically the offset distances are between 0.1 and 12 inches. In a rotating blade test, the measurement system must not interfere with the flow. Displacement lasers would not meet this criterion. However, this is the only known drawback and the state of the field is progressing quickly. It is anticipated that a large standoff laser with high accuracy will be available within a few years.

There are several methods used by displacement lasers. Some are based on the intensity of the returned light. Some are based on reflection. Some are based on diffusion-reflection. Because of the curved nature of blades, two important properties must be considered in selecting a laser type for blade applications. First, the point of reflection must not vary as the target vibrates. Second, low sensitivity to target orientation angle is required.

The method selected for this application is the diffusion-reflection method. These lasers are best suited for diffusive type surfaces, including metals. In this method, a beam is emitted perpendicular to the target. The reflection is diffused in all directions, with some of the reflected light hitting the receiver lens (Figure 1). Based on the return angle, the receiver lens focuses the returned light to a point on a photo-sensitive device. Through calibration, displacement can be determined as the reflection angle is proportional to target distance. The point of reflection does not vary with target distance. This results in low sensitivity to variability in target angle. Typical sensitivity for a diffusion-reflection laser would be 1% error for ±10° angle change.

The Keyence LC-2450 was used in implementing this work[12]. The LC-2450 is a diffusion-reflection type displacement sensor. Some key specifications for the LC-2450 are given in Table 1.

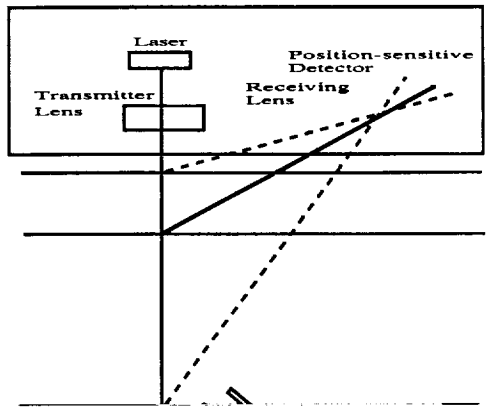

Figure 1: Schematic of Operating Principles of a Diffusion-Reflection Displacement Laser.

Specification	Value
Measuring Range	± 8 mm (± 0.31in)
Mean Standoff Distance	50 mm (1.97 in)
Typical Resolution	0.5 μm (1.97 μ-in)
Frequency Response	20 kHz
Sampling Frequency	50 kHz
Instantaneous Response Time to within ±10%	100 μs

Table 1: Specifications for a Displacement Laser

Laser Doppler Velocimeters

The considerations for selecting an LDV system are similar to those for selecting a displacement laser. The key decision is whether to use a tracker system or a counter system. A tracker closes a loop around the received Doppler signal and outputs the closed loop values. This provides clean signals given a continuous Doppler signal. Because of the closed loop nature, the does not begin to output until the signal is "locked". This time, although small, is not suitable for short burst information as in rotating systems.

A counter uses a very accurate clock to time the Doppler signal cycles. From this, the frequency and velocity are derived. The counter can respond very fast if it is set to count only one Doppler signal period. Response times can be applicable to high speed turbomachinery applications. However, at these rates, the noise is prohibitively high for accurate measurement. In order to get sufficiently reduced noise, the counter must be set to the speed of a tracker.

Based on the above discussion, it is clear that LDV systems cannot be used for high speed rotating applications. However, the use of LDV systems for stationary strain are demonstrated in this report.

The Dantec 55X in conjunction with a Dantec 55N10 Frequency Shifter and 55N20 Tracker were selected for this application[13]. Some key specifications for the Dantec 55X system are given in Table 2.

Specification	Value
Measuring Range	~±0.1 m
Mean Standoff Distance	Multiples of 1.0 m
High End Resolution	36 μm/sec – 11 mm/sec
Full Range	±4.6 mm/sec – ±1.4 m/sec
Frequency Response	1200 kHz

Table 2: Specifications for a Laser Doppler System

LASER MEASUREMENT TO STRAIN: THEORY

This section details equations and theory required to derive strain from the laser measurements. First the strain equations are shown given a set of continuous displacement measurements x(t). In rotating systems, in which the data is sparse, it is first necessary to measure or develop the displacement time histories, x(t).

Strain from Displacement

Assume the displacement time histories at N physical points are measured. This defines the displacement state of these N points. A modal matrix, $\Phi \in R^{NxN}$, containing these N points and N modes of interest is used as a filter or operator to obtain the modal displacements of the N modes:

$$q(t) = \Phi^{-1}x(t) \tag{1}$$

Equation (1) defines the modal displacements. From this another modal transformation, $\Phi' \in R^{MxN}$, having the same N modes but M strain outputs can be developed and used to determine the strain at any location on the structure, in particular the root of the blade. Equation 8 shows this.

$$\varepsilon(t) = \Phi' q(t) \tag{2}$$

Equation 2 defines the strain at M locations of interest.

While displacement lasers measure x(t) directly, the LDV system measure velocity and x(t) must be derived. In the special case of harmonic response, this is not a problem. The LDV velocity signal can be used to derive strain. Similar to equation 1, the modal velocities can be derived from the velocity measurements:

$$\dot{q}(t) = \Phi^{-1}\dot{x}(t) \tag{3}$$

Using harmonic identities, we can find q(t) without integration and equation 2 can be applied for strain:

$$q(t) = \frac{1}{p}\Phi^{-1}\dot{x}(t - \pi/2p) \tag{4}$$

Continuous Signal from Sparse Rotating Data

For a stationary object, the analog signal from the laser is continuous and the displacement time history, x(t), is read directly (this section will assume a displacement laser). However, for rotating blades, the measurements are a set of evenly spaced clusters of measurements (Figure 2). Clearly, just connecting the sampled data points is not sufficient to define the full time history, x(t). To overcome this limitation, a method for representing x(t) as a continuous function from the sampled points $x_k = x(t_k)$ is derived.

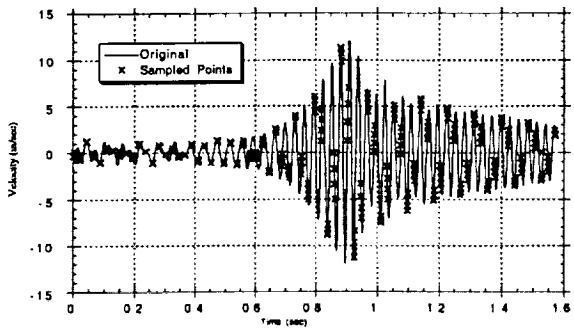

Figure 2: When measuring rotating blades, sampled data points do not directly provide a complete time history.

The development begins be recalling that any periodic function can be expanded in a Fourier Series as:

$$\hat{f}(t) = \sum_{i=0}^{N} [a_i \cos(\omega_i t) + b_i \sin(\omega_i t)] \qquad (5)$$

where:

$$\omega_i = \frac{2\pi i}{T}, \qquad T = t_N - t_0$$

and $\hat{f}(t)$ represents a function f(t) rebuilt from its frequency decomposition.

For a given sample, T and N are known so the $\{\omega_i\}$ are known. If the coefficients $\{a_i\}$ and $\{b_i\}$ are known, then the function is known over the entire measurement domain. For a continuous evenly spaced set of data, $\{a_i\}$ and $\{b_i\}$ are found via a fast Fourier transform (FFT). The problem is not so simple for the clustered data of the rotating blade problem.

The coefficients $\{a_i\}$ and $\{b_i\}$ are found from the set of sampled data $\{f(t_k) : k=1,..,N\}$ by the solution to:

$$\begin{bmatrix} \cos\omega_0 t_1 & \cdots & \cos\omega_N t_1 & \sin\omega_1 t_1 & \cdots & \cos\omega_N t_1 \\ \vdots & & \vdots & \vdots & & \vdots \\ \vdots & & \vdots & \vdots & & \vdots \\ \vdots & & \vdots & \vdots & & \vdots \\ \vdots & & \vdots & \vdots & & \vdots \\ \cos\omega_0 t_N & \cdots & \cos\omega_N t_N & \sin\omega_1 t_N & \cdots & \sin\omega_N t_N \end{bmatrix} \begin{Bmatrix} a_0 \\ \vdots \\ a_N \\ b_1 \\ \vdots \\ b_N \end{Bmatrix} = \begin{Bmatrix} f(t_1) \\ \vdots \\ \vdots \\ \vdots \\ f(t_N) \end{Bmatrix} \qquad (6)$$

This is equivalent to the common form Ax=b, which represents a linear system of equations with constant coefficients.

Recall that ω_i and t_i are known, so the terms of the matrix A can be evaluated. The solution to the problem is not as direct as one might hope. In order to maintain a real time system, this solution must be fast—on par with the O(NlogN) FFT. This eliminates the basic but costly Gauss elimination which is $O(N^3)$ and the super-robust singular value decomposition which is $O(N^3)$. Also, due to the clustered nature of the data, error propagation is a serious concern. This eliminates many other techniques such as the basic QR which suffers in the calculation of R^{-1}. Fortunately, other solution techniques exist which take advantage of the structure of the problem to enable a quicker and more accurate solution.

IUQR Algorithm

One solution technique that is particularly useful for a solution to the coefficients of Equation 5 is the inverse unitary QR (IUQR) algorithm.[14] The IUQR algorithm does not explicitly form Equation 6, but casts the problem of Equation 5, defined over the domain $\Theta \in [0,2\pi)$ into a complex problem over the complex domain $z=e^{i\theta}$. Then there is a solution to the complex problem:

$$DAc = D\Lambda^{1}f \qquad (7)$$

where: $D = \text{diag}[w_1, w_2, ..., w_m]$ and w_k is a positive weight on $f(t_k)$, with $m \le N$

$\Lambda = \text{diag}[z_1, z_2, ..., z_m]$

f = vector of data points

$$A = \begin{bmatrix} 1 & z_1 & z_1^2 & \cdots & z_1^{N-1} \\ 1 & z_2 & z_2^2 & \cdots & z_2^{N-1} \\ \vdots & \vdots & \vdots & \vdots & \vdots \\ \vdots & \vdots & \vdots & \vdots & \vdots \\ 1 & z_m & z_m^2 & \cdots & z_m^{N-1} \end{bmatrix}$$

The solution, c, contains the coefficients for the least squares solution to Equation 6. The details of the algorithm are complicated and are found in Ref. 14. Simply put, the algorithm uses Szego polynomials and the structure of the problem to construct a solution directly without explicitly forming Q or R^{-1} as would be needed for most QR decompositions.

The IUQR algorithm is $O(pN^2)$, where p is some coefficient. Due to the complex arithmetic and the large number of calculations within each loop, the coefficient p is fairly high, say 40. Therefore, for small problems the IUQR routine acts like $O(N^3)$ but as N gets larger than 100, it acts as $O(N^2)$. While not O(NlogN) like the FFT, this is near real time.

The IUQR algorithm is used as the basis for real time solutions of Equation 6. From this the continuous function is defined over the entire measurement domain using Equation 5.

LASER MEASUREMENT TO STRAIN: PRACTICAL CONSIDERATIONS

The theory of a laser strain measurement system is very simple as shown in Equations 1 through 6. Implementation is much more complicated. This section details the key issues and identifies solutions for each. The section shows that making the laser strain measurement system work in practice is a difficult endeavor, but with patience, practice, and sound judgement, good strain results may be obtained.

Dynamic Range and Noise

Evenly spaced data is subject to the Nyquist criteria for expansion by Fourier Series. The Nyquist frequency is 1/2 the sample frequency. Equation 5 is also subject

to the Nyquist criteria. In this case, the Nyquist frequency 1/2 of the average sample frequency. This frequency is given by N/T (see Equation 5). This suggests that the blade should be maximally sampled each time it comes into view. Theoretically, this will maximize the ratio N/T and the dynamic range. Practically, it is not possible.

The practical limits due to noise are based on the choice of algorithm to solve Equation 5. It has been shown previously that instability due to noise increases as the cluster size increases[15]. Instability due to noise was also repeatedly observed during testing for this report. Experience leads to three axioms needed for practical implementation of the IUQR (or any other) algorithm on clustered data.

Axiom 1: *Measurement noise must be minimized.*

Axiom 2: *The process being measured must be band limited to a frequency below the effective Nyquist frequency of the measurements since higher frequency responses will alias as noise into the solution.*

Axiom 3: *End point matching is required to prevent end point mismatches from creating high frequency content that acts as noise in the solution. Windowing may be used to achieve end point matching.*

Cluster Size

It is not noise alone that creates the instability in the algorithms. It is noise coupled with the cluster size. Noise sensitivity increases with cluster size. Given that noise will exist, there is a maximum cluster size that will result in a stable solution. This maximum cluster size is dependent on several practical aspects such as the size of the matrix A in Equation 6, laser noise level, and the algorithm chosen to solve Equation 5. Because of this specific nature of these items, a general, rather than theoretical, methodology is developed to determine the cluster size.

First, define "in-view ratio" as the percent of time that the blade is in view. The reciprocal of the in-view ratio, which is typically the number of blades, has greater physical significance that the in-view ratio.

The methodology begins with a wide band time history similar to that shown in Figure 3. This is assumed to represent some real vibration data. A set of blade counts and associated cluster sizes are selected for study. The signal is then sampled and the IUQR scheme is used to recreate the full filtered signal. For a given blade count, a cluster size of 1 (uniform spacing) is used as the baseline since the algorithm is very stable for a cluster size of 1 (just as the FFT is stable in this condition). The metric for comparison is the ratio of the norm of the solution vector, |x|, to the norm of the solution vector for a cluster size of 1.

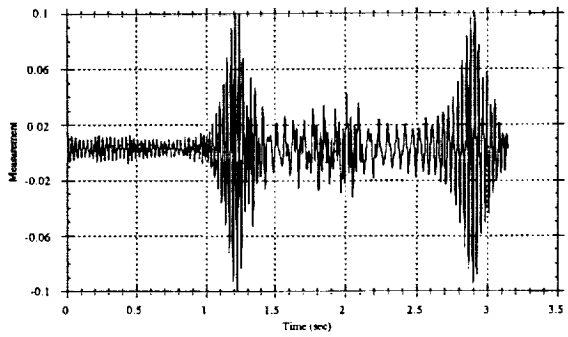

Figure 3: Typical wide band time history used to determine limits on cluster size

For the test apparatus used in this experiment, the maximum cluster size was determined by sampling the data in cluster sizes from 1 to 10 in blade counts from 2 to 25. Figure 4 shows the results.

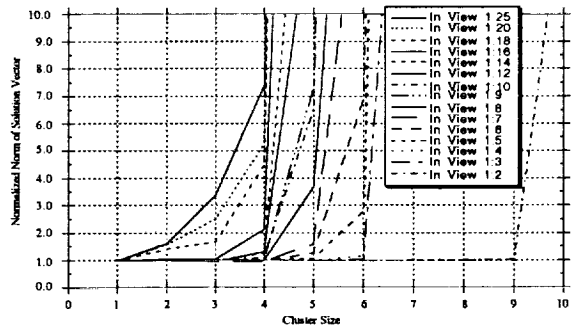

Figure 4: Stability of IUQR algorithm in use with the LC-2450 displacement and blade counts and cluster sizes.

The steep slopes on the curves in Figure 4 show how quickly the solution becomes unstable. The corner points from these curves have been plotted in Figure 5. This figure is the ultimate reference guide for this method. The blade configuration will govern how large of a cluster size can be used. This in turn governs the maximum frequency that can be resolved and this is shown on the Y2 axis of Figure 5. Remember, signal must be band limited by this value.

For all practical purposes, a cluster size of 1 is not very useful since it only can resolve frequencies at 0.5*RPM. A cluster size of 2 may be acceptable since it can resolve up to the RPM frequency. This captures all of the once per rev information. However, this limit is so close to the main excitation frequency that it makes the regeneration suspect. Therefore, a minimum

cluster size of three is suggested. Looking at Figure 5, this implies that this method is only useful for fan with less than 16 blades. This limitation must be accepted.

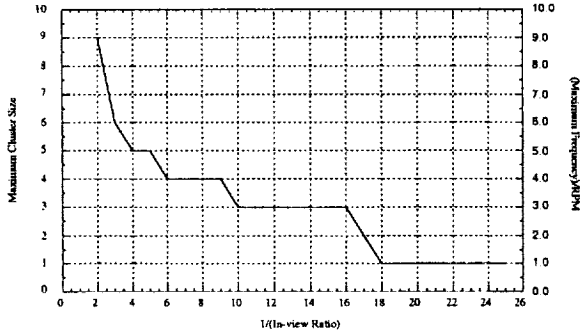

Figure 5: Cluster size limitation for different blade counts

Determination of Modal Content

Since the method described here is a modal transformation method, all of the usual modal representation issues are relevant. One important issue is the number of modes required to represent both the measured quantity (displacement or velocity) and the strain output. There have been volumes of data and theories presented on this. That is beyond the scope of this paper. The nature of blades is such that the strain is typically governed by three or four modes. For this research, two lasers were available so two modes were considered.

Selection of Measurement Location Points

This may be the most important aspect of using a finite set of lasers to determine strain. There are actually two aspects related to measurement location. The first is choosing optimal locations for measurement (this section) and the second is determining which location is actually being measured (next section).

The strain derivation methodology requires that the displacement measurements be accurately transformed into modal amplitudes. While the mode shapes are inherently orthogonal, this quality is typically lost at a small subset of points. The dynamicist must choose measurement points so that the matrix Φ in Equation 1 is as orthogonal as possible. The loss of independence results in amplification of any noise or any uncertainty in the modal amplitudes.

For example, consider the flared twin-blade design shown in Figure 6. The Y axis is the rotation axis. The first two modes of each uncoupled blade are shown in Figure 7. These are classic bending and torsion.

In order to derive the strain using a two mode approach, two lasers are needed. A subset of potential laser points is shown in Figure 8. Any pair of these may be used. Also shown in Figure 8 are the modal matrices associated with combinations of these points. As can be seen by the normalized determinants, the (3,4) combination is an excellent choice for laser locations and (1,2) is an unacceptable choice. Set (5,3) is ambiguous, and the derived strain using this combination (Figure 9) shows just this. Clearly, noise has been amplified and the importance of a good choice of locations has been shown.

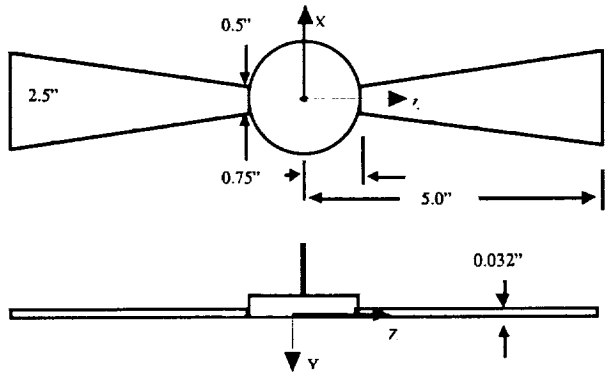

Figure 6: Schematic of flared blade and attached.

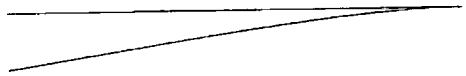

(a) Mode 1, 1st out of plane bending, f = 31.7 Hz

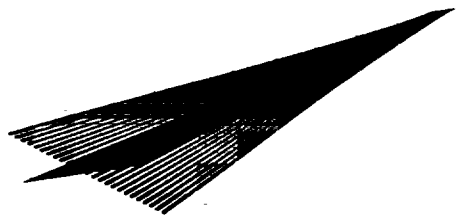

(b) Mode 2, torsion, f = 160 Hz

Figure 7: First two mode shapes of the flared blade.

Unfortunately, for a rotating system, the lasers must be on the structure at the same time during the entire blade passage. Hence, they must be in radial line, as in locations (1,2) or (5,3) in Figure 9. This implies that more than two lasers are needed to clearly and cleanly distinguish between the first two modes in this rotating model. This understanding is critical to getting good results.

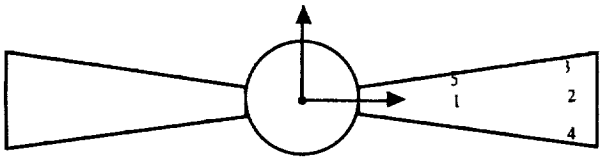

(a)

$$\Phi_{21} = \begin{bmatrix} -176.7 & 0.0 \\ -30.50 & 0.0 \end{bmatrix}, \quad \left|\overline{\Phi}_{21}\right| = 0.00$$

$$\Phi_{34} = \begin{bmatrix} -168.4 & -292.0 \\ -168.4 & 292.0 \end{bmatrix}, \quad \left|\overline{\Phi}_{34}\right| = 2.00$$

$$\Phi_{35} = \begin{bmatrix} -168.4 & -292.0 \\ -26.98 & -66.52 \end{bmatrix}, \quad \left|\overline{\Phi}_{35}\right| = 0.07$$

(b)

Figure 8: (a) Potential measurement locations on the flared blade; (b) their associated modal matrices and normalized determinants.

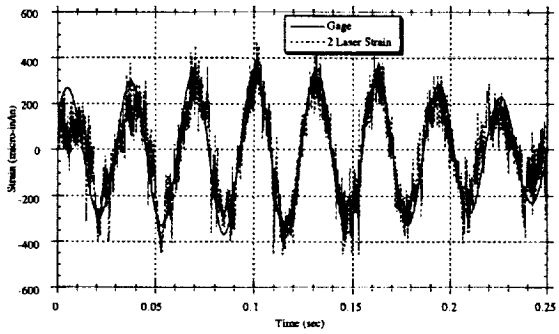

Figure 9: Demonstration of the noise amplification by choosing a weakly independent input modal matrix.

Measurement Point Identification

As shown in Equation 1, the mode shape coefficient at the laser measurement location is used in the transformation to strain. Because of this, the accuracy of the measurement location is important. It is easy to show that a small (±0.1 inch) errors in laser locations can result in a large (20%) errors in strain. Therefore, some care must be taken in identifying the measurement locations. Careful measurement may be complicated because some lasers do not come to a perfect point when in focus. Therefore, determining locations via direct measurement can easily result in large percentage errors.

To alleviate this problem, a procedure was developed to determine the laser measurement locations without measurement. First the system is excited at a resonance for each laser used. For N lasers, the steady state responses to N resonant excitations are recorded. For an assumed measurement location, the modal amplitudes can be calculated using Equation 1. N measurements results in N modal amplitude time histories corresponding to N modes. These time histories are reduced to a single value via root mean square summation of the time history. Now a single value represents each modal amplitude. In equation form,

$$q_{i,rms} = \sqrt{\sum_{t=1}^{m} q_t^2} \qquad i = 1, \ldots, N \qquad (8)$$

where the subscript t spans a set of m points in time.

For the excitation at ω_i, $q_{i,rms}$ should dominate. Therefore, we look for a set of N locations where $q_{1,rms}$ dominates at ω_1, $q_{2,rms}$ dominates at ω_2, and so on. This process can be achieved quickly if an approximate location for each laser is considered. The search is across an N dimensional matrix of cases.

Rigid Body Compensation

Strain is a relative displacement quantity. The lasers measure absolute motion. The difference can negligible if there is a nearly fixed condition somewhere in the modeled structure. However, in the case of a test system excited by a shaker, the base cannot be considered fixed. This rigid body motion must be considered in some way. Recalling that it requires one laser for each degree of freedom, considering all six rigid body degrees of freedom may not be practical. It is recommended that only the likely rigid body motions be considered and compensation be applied only to these motions.

It must be pointed out that there are exceptions to the need for rigid body compensation. However, the structural dynamicist can use his system knowledge to eliminate this need. Specifically, even if the system is fixed to a shaker, if the input is resonant and the damping is low, then the rigid body (base) motion will be small compared to the total measurement. In this case, errors are expected to be less than 2%. Contrast this to the off-resonant excitation where the rigid body error may be as high as 50%. The authors believe the failure to compensate for this is the reason several previous laser strain systems have failed.

RESULTS: NON-ROTATING FLAT BLADE

This section describes use of the displacement laser and LDV strain measurement system on non-rotating systems. While this was demonstrated for a resonant condition [Ref. 11], this section extends the procedure to multiple modes, off-resonant conditions, and non-stationary excitations.

A simple beam is used as an example. This beam is part of a blade-hub system as shown in Figure 10. The first two modes are the classic first and second bending of a beam. The hub is connected to a shaker to provide excitation. The practical issues of the previous section were addressed prior to taking data.

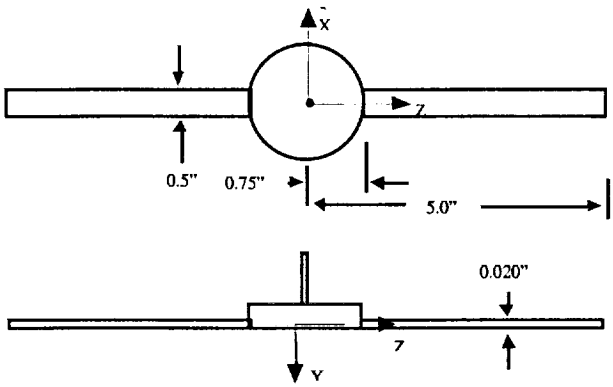

Figure 10: Schematic of flat blade and attached hub

Resonant Strain

As a reference to judge the laser strain system, a strain gage was placed near the hub of the blades. This gage measurement is used as the reference in all plots. By far the easiest condition under which to determine laser strain is at a resonant condition. This condition has two huge advantages: Rigid body effects are minimized and a single mode dominance. Figure 11 shows a comparison of the strain gage and the LDV laser derived strain given a first natural frequency base input at the first natural frequency. This figure shows the strain derived using only the first mode and then using the first two modes. Clearly all three are very close. This implies that one laser and one mode could be used for this resonant condition. Most importantly, the transformation from laser velocity to strain is demonstrated.

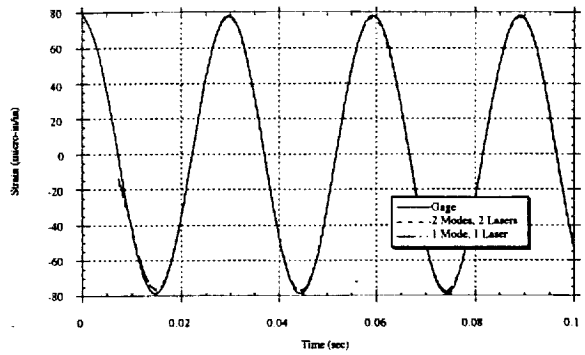

Figure 11: A comparison of the strain measured by a strain gage and the strain derived from a one laser LDV system and a two laser LDV system. The excitation is harmonic at the first natural frequency (35 Hz). Rigid body compensation was not applied.

A similar result can be shown for the second mode (Figure 12). In this case, there is a small contribution from the first mode (35.0 Hz) contaminating the one mode laser results. Also, rigid body effects are coming into play. Similar results are demonstrated for the displacement laser system in Figures 13 and 14. The conclusion from this data is that a rigid body correction is not required for resonant excitation. A single mode solution, implying a single measurement, is possible but only with very pure signals.

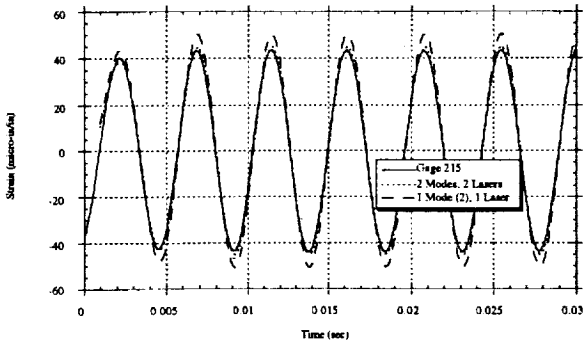

Figure 12: A comparison of the strain measured by a strain gage and the strain derived from a one laser LDV system and a two laser LDV system. The excitation is harmonic at the second natural frequency (215 Hz). Rigid body compensation was not applied.

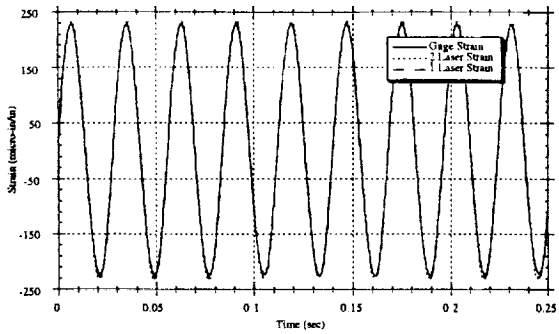

Figure 13: A comparison of the strain measured by a strain gage and the strain derived from one displacement laser and two displacement lasers. The excitation is harmonic at the first natural frequency (35.0 Hz). Rigid body compensation was not applied.

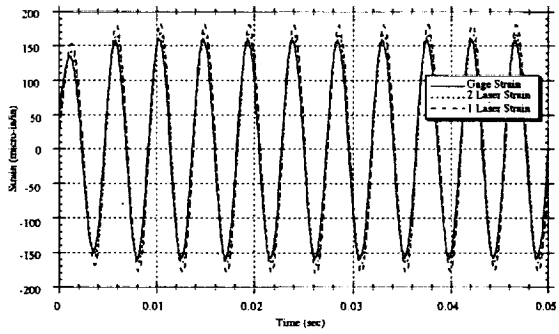

Figure 14: A comparison of the strain measured by a strain gage and the strain derived from one displacement laser and two displacement lasers. The excitation is harmonic at the first natural frequency (215 Hz). Rigid body compensation was not applied.

Off-resonant Oscillation

Off-resonant response is far more complex than resonant response because two issues become important. First, a multi-mode approach must be taken since many modes are contributing significantly to the response. Second, rigid body compensation is required because the amplification (response to excitation) is not very large. As mentioned before, extra measurements are needed for each rigid body degree of freedom.

As an example of the importance of a rigid body compensation, consider an off-resonance response. In the simple blade example, a 36.2 Hz harmonic excitation is used rather than the 35.0 Hz resonant excitation of the previous section. Figure 15 shows a comparison of the strain gage strain and the LDV laser derived strain using two lasers without considering the rigid body correction. The error between peaks is an unacceptable 27%. The excitation is from an axial shaker imposing a transverse (Y-axis) translation and a out-of-plane (X-axis) rotation into the base of the blade. When rigid body compensation is applied to these two degrees of freedom via two more laser measurements, the error drops to 5% (Figure 16). Similar results can be demonstrated for the displacement laser system.

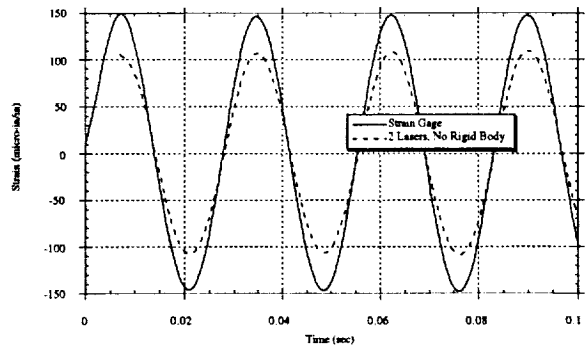

Figure 15: A comparison of the strain measured by a strain gage and the strain derived from the two laser LDV system. The excitation is off-resonance and harmonic. No rigid body compensation was applied.

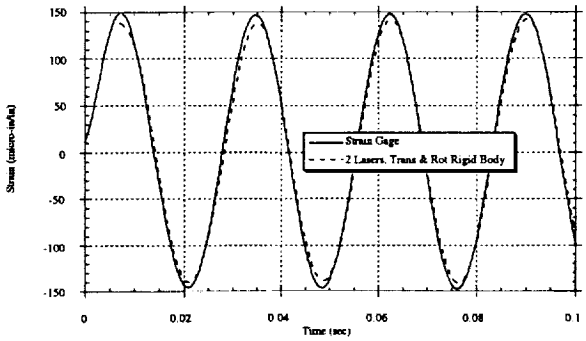

Figure 16: A comparison of the strain measured by a strain gage and the strain derived from the two laser LDV system. The excitation is off-resonance and harmonic. Rigid body compensation was applied.

RESULTS: ROTATING BLADE SYSTEM

The full demonstration of rotating strain has not been completed. However, high speed data acquisition has been demonstrated. The requirements for rigid body compensation and for a flared blade are more than two

lasers. Only two lasers were available at test time. The rotating blade used is shown in Figure 6.

Based on Figure 5 and the dimensions of the flared blade, a cluster size of 3 is the maximum possible. With this in mind, the blade pair was rotated up to 2400 RPM.

Two lasers were used in this demonstration. Laser 1 (called the tip laser) is 3.53" from the axis of rotation and laser 2 (called the mid laser) is 1.88" from the axis of rotation. Figure 17 shows a small time segment of the laser measurements from the rotating structure. The measured data of Figure 17 is reduced to 3 points per blade passage. This is shown in Figure 18.

Figures 17 and 18 show that the technology exists to record displacement data at high data rates. Given enough laser measurements, this data can then be converted to strain. The process from this point is to perform rigid body compensation on the data, use the IUQR algorithm to expand the discrete measurements into a full field, and use Equations 1 and 5 to derive a continuous strain measurement.

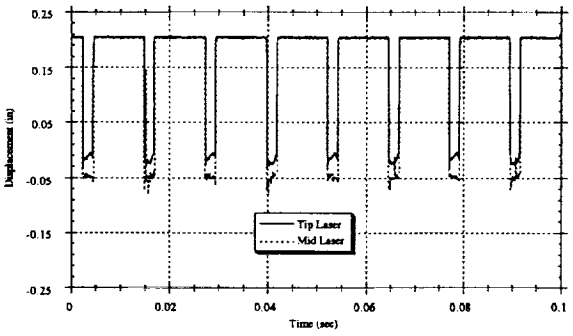

Figure 17: View of rotating data recorded by two lasers on the flared blade. Note that this represents both blades.

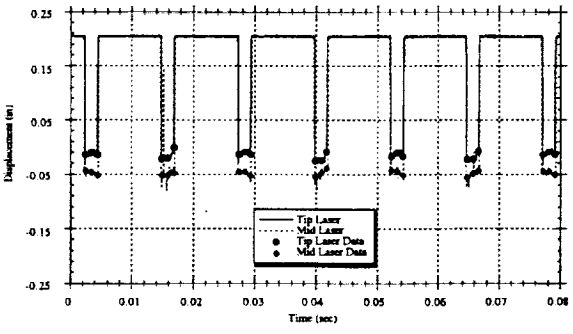

Figure 18: Data measurement points extracted from the rotating data for use in determining the strain.

SUMMARY AND CONCLUSIONS

The work presented here demonstrates that displacement laser based systems can be used to measure the strain in stationary systems. Differences between the laser derived strain and the reference strain gage were consistently less than 1% for resonant conditions and less than 10% for other conditions. Analytic demonstration of the method to rotating systems has been provided. Demonstration of the method for rotating systems has yet to be completed.

The theory also demonstrates that the sparse number of points measured by the lasers as the blades move past can be expanded, under certain conditions, into the complete strain field. Furthermore, this can be done at near $O(N^2)$ speed. This is near real time on a high end computer.

Beyond theory, this work identifies several practical issues for any laser system and demonstrates implementation techniques to overcome these issues. It has been shown that practical laser based strain measurement is possible with proper attention.

Finally, given the current state of this development, displacement lasers can be confidently used to measure the strain in stationary systems in a non-contacting way. However, further advances are required in order to get to high resolution (as exists today) with sufficient stand-off so that this system can become truly non-interfering.

LITERATURE CITED

1. Fahy, F.J., "Apparatus for the Required Assessment of High Speed Flutter Model Stability", Journal of Sound and Vibration, Vol. 12, No. 2, pp. 33-36, 1965.
2. Fan, Y.C., M.S. Ju, and Y.G. Tsuei, "Experimental Study on Vibration of a Rotating Blade", Transactions of the ASME, Vol. 116, July 1994, pp. 672-677.
3. Staeheli, W., "The Measurement of the Vibrations of Rotor Blades in Turbomachines—An Inductive Meaurement Procedure", VDI-Z, Vol. 117, No. 20, Oct. 1975.
4. Haupt, U. and M. Rautenberg, "Blade Vibration Measurements on Centrifugal Compressors by Means of Telemetry and Holographic Interferometry", Transactions of the ASME, Vol. 106, January 1984, pp. 70-78.
5. Carlsson, Tergny E., "Measurement of Three-dimensional Shapes Using Light-in-Flight Recording by Holography", Optical Engineering, Vol. 32 No. 10, October 1993, pp. 2587-2592.

6. Oliver, D.E., "Principles and Applications of SPATE--An Update", Procedings of the SEM Spring Conference on Experimental Mechanics, 1990.
7. Kurkov, Anotole P., "Optical measurement of Unducted Fan Blade Deflections", NASA Technical Memorandum 100966, 1989.
8. McCarty, P.E., J.W. Thompson, and R.S. Ballard, "A non-Interference Technique for Measurement of Turbine Engine Compressor Blade Stress", Proceedings of the AIAA/SAE/ASME 16th Joint Propulsion Conference, Hartford, Connecticut, June 30-July 2, 1980. AIAA-80-1141.
9. Chi, Ray M., and Henry T. Jones, "Demonstration Testing of a Noninterference Technique for Measuring Turbine Engine Rotor Blade Stresses", Proceedings of the AIAA/ASME/SAE/ASEE 24th Joint Propulsion Conference, Boston, Massachusetts, July 11-13, 1988. AIAA-88-3143.
10. Kadambi, J.R., R.D. Quinn, and M.L. Adams, "Turbomachinery Blade Vibration and Dynamic Stress Measurements Utilizing Nonintrusive Techniques", Transactions of the ASME, Vol. 111, October, 1989, pp. 468-474.
11. Reinhardt, A.K., J.R. Kadambi, and R.D. Quinn, "Laser Vibrometry Measurements of Rotating Blade Vibrations", Transactions of the ASME, Vol. 117, July, 1995, pp. 484-488.
12. Keyence Corporation, "LC-2400 Series Instruction Manual", Japan, 1994.
13. DANTEC Documentation Department, "Instruction and Service Manual: 55X Laser Vibrometer", 1983.
14. Reichel, L, G.S. Ammar, and W.B. Gragg, "Discrete Least Squares Approximation by Trigonometric Polynomials", Center for Computational Studies, University of Kentucky, CCS-90-2, 1990.
15. Linden, D.A., "A Discussion of Sampling Theorems", Proceedings of the IRE, July 1959, pp.1219-1226.